

INTERLEAVED DIMENSION DECOMPOSITION: A NEW DECOMPOSITION METHOD FOR WAVELETS AND ITS APPLICATION TO COMPUTER GRAPHICS

Manfred Kopp and Werner Purgathofer
Vienna University of Technology
Institute of Computer Graphics
Karlsplatz 13/186-2
Vienna, Austria
{ kopp | wp } @cg.tuwien.ac.at
<http://www.cg.tuwien.ac.at/home/>

ABSTRACT

Wavelets in 2D or higher dimensions are often generated by a decomposition scheme from 1D wavelets. There are two decomposition schemes called the standard and the nonstandard decomposition which are used in most applications of higher dimensional wavelets. This paper introduces a new decomposition method, the interleaved dimension decomposition and compares its advantages and disadvantages with the other decompositions. Based on the properties of the interleaved dimension decomposition, applications to computer graphics are sketched including multiresolution painting, morphing in 2D and 3D, and image compression.

Keywords: Wavelets, morphing, multiresolution painting, image compression

1. INTRODUCTION

In the last years, wavelets have become a popular research topic in various fields of computer graphics. The different applications of wavelets in computer graphics include wavelet radiosity [Gortl93], multiresolution painting [Berma94], curve design [Finke94], mesh optimization [Eck95], volume visualization [Lippe95], image searching [Jacob95], animation control [Liu94], BRDF representation [Schrö95], and, one of the first applications in computer graphics, image compression [Shapi93]. As it is noticed in the preamble of [Glass95], wavelets and wavelet transforms can become as important and ubiquitous in computer graphics as spline based techniques are now.

In this paper a new decomposition for separable higher dimensional wavelets is introduced and compared with the standard and nonstandard decomposition. Chapter 2 describes the wavelets in 1D. In chapter 3 traditional extensions to higher dimensional wavelets including matrix dilation methods, standard and nonstandard decomposition are discussed. Chapter 4 introduces the new interleaved dimension decomposition and compares it

with traditional approaches. Chapter 5 shows some computer graphics applications of the interleaved dimension decomposition.

2. WAVELETS IN 1D

This chapter gives a very short introduction in the theory of wavelets. A more detailed discussion of this topic can be found in [Daube92].

2.1 Orthonormal Wavelets

The orthonormal wavelet transform is based on two functions $\psi(x)$ and $\phi(x)$, which have the properties:

$$\int \phi(x) dx = 1; \quad \int \psi(x) dx = 0 \quad (1)$$

These functions with their translations and dilations $\psi_{j,k}(x)$ and $\phi_{j,k}(x)$ build an orthonormal basis and therefore any function in $L^2(\mathbb{R})$ can be reconstructed with these basis functions. $\phi(x)$ is called scaling- or smooth-function, and $\psi(x)$ wavelet or detail function. $\psi_{j,k}(x)$ and $\phi_{j,k}(x)$ can be constructed from

their mother functions $\psi(x)$ and $\phi(x)$ in the following manner:

$$\begin{aligned}\phi_{j,k}^j(x) &= \sqrt{2^j} \phi(2^j x - k), \\ \psi_{j,k}^j(x) &= \sqrt{2^j} \psi(2^j x - k), \quad j, k \in Z\end{aligned}\quad (2)$$

$\{\phi_{j,k}^j / k \in Z\}$ form an orthonormal basis of functions in vector space V^j . These vector spaces are nested, that is, $V^0 \subset V^1 \subset V^2 \subset V^3 \subset \dots$. Given a function $f(x)$ over $[0,1]$, this function can be approximated in V^j with 2^j scaling coefficients s_k^j :

$$f^j(x) = \sum_{k=0}^{2^j-1} s_k^j \phi_{j,k}^j(x) \quad (3)$$

Let $\langle f(x), g(x) \rangle$ denote the inner product of the function $f(x)$ and $g(x)$ with:

$$\langle f(x), g(x) \rangle = \int_{-\infty}^{+\infty} f(x) g(x) dx \quad (4)$$

The scaling coefficients s_k^j can be computed by the inner product of the function $f(x)$ and the corresponding scaling function $\phi_{j,k}^j(x)$:

$$s_k^j = \langle f(x), \phi_{j,k}^j(x) \rangle \quad (5)$$

Also the detail functions $\{\psi_{j,k}^j / k \in Z\}$ form an orthonormal basis of functions in the detail vector space W^j , which is the orthogonal complement of V^j in V^{j+1} . W^j can be thought of as containing the detail in V^{j+1} , which can not be represented in V^j . The vector space V^{j+1} can be decomposed in the following manner:

$$\begin{aligned}V^{j+1} &= V^j \oplus W^j = V^{j-1} \oplus W^{j-1} \oplus W^j = \dots \\ &= V^0 \oplus W^0 \oplus W^1 \oplus \dots \oplus W^j\end{aligned}\quad (6)$$

Let d_k^j be the wavelet or detail coefficients, given through:

$$d_k^j = \langle f(x), \psi_{j,k}^j(x) \rangle \quad (7)$$

then $f^j(x)$ can be calculated from the wavelet coefficients $\{d_k^j / i < j\}$ and the scaling coefficient s_0^0 as follows:

$$\begin{aligned}f^j(x) &= f^{j-1}(x) + \sum_{k=0}^{2^{j-1}-1} d_k^{j-1} \psi_{j-1,k}^{j-1}(x) \\ &= s_0^0 \phi_{0,0}(x) + \sum_{m=0}^{j-1} \sum_{k=0}^{2^m-1} d_k^m \psi_{m,k}^m(x)\end{aligned}\quad (8)$$

The calculation of the coefficients $\{s_0^0, d_k^i / 0 \leq i < j; 0 \leq k < 2^i\}$ from the scaling coefficients $\{s_k^j / 0 \leq k < 2^j\}$ is called wavelet transformation. The fast wavelet transformation uses a pyramid scheme with two subband filters, the smoothing or scaling filter (h_m), and the detail or wavelet filter (g_m). In one transformation step the 2^i scaling coefficients s_k^i are replaced by 2^{i-1} scaling coefficients s_k^{i-1} and 2^{i-1} wavelet coefficients d_k^{i-1} :

$$s_k^{i-1} = \sum_m h_{2k-m} s_m^i; \quad d_k^{i-1} = \sum_m g_{2k-m} s_m^i \quad (9)$$

This step is repeated on the remaining scaling coefficients, until s_0^0 is computed. The reconstruction step can be performed using the adjoint filtering operation:

$$s_k^i = \sum_m h_{k-2m} s_m^{i-1} + g_{k-2m} d_m^{i-1} \quad (10)$$

The whole reconstruction of the scaling coefficients s_k^i from s_0^0 and the wavelet coefficients of various resolutions is called inverse wavelet transformation.

2.2 Biorthogonal Wavelets

Biorthogonal wavelets use scaling basis functions $\phi_{j,k}(x)$ which are not orthogonal. Therefore the scaling coefficients can not be computed by Eq. 5. But it can be shown, that for every basis $\{\phi_{j,k}(x)\}$, which is called primal basis, there is a dual basis $\{\tilde{\phi}_{j,k}(x)\}$ and the scaling coefficient can be computed by:

$$s_k^j = \langle f(x), \tilde{\phi}_{j,k}(x) \rangle \quad (11)$$

In analogy, the detail coefficient d_k^j can be computed by the inner product of the function $f(x)$ and the corresponding dual wavelet function $\tilde{\psi}_{j,k}(x)$:

$$d_k^j = \langle f(x), \tilde{\psi}_{j,k}(x) \rangle, \quad (12)$$

The following conditions must be satisfied between the primal scaling and wavelet functions and their dual counterparts:

$$\begin{aligned}
\langle \phi_{jk}(x), \tilde{\phi}_{j,l}(x) \rangle &= \delta_{k,l} \\
\langle \psi_{jk}(x), \tilde{\psi}_{j,l}(x) \rangle &= \delta_{k,l} \\
\langle \phi_{jk}(x), \tilde{\psi}_{j,l}(x) \rangle &= 0 \\
\langle \psi_{jk}(x), \tilde{\phi}_{j,l}(x) \rangle &= 0
\end{aligned} \tag{13}$$

The fast wavelet transformation with biorthogonal wavelets uses the dual filter pair (\tilde{h}_m) and (\tilde{g}_m) corresponding to the dual basis functions. Therefore a wavelet transformation step uses the following formula instead of Eq. 9:

$$s_k^{i-1} = \sum_m \tilde{h}_{2k-m} s_m^i; \quad d_k^{i-1} = \sum_m \tilde{g}_{2k-m} s_m^i \tag{14}$$

The fast inverse wavelet transformation with biorthogonal wavelets uses the primal filter pair (h_m) and (g_m) , hence the procedure is the same as for orthogonal wavelets (Eq. 10). If the primal and dual basis functions and filters are exchanged with each other, the result is also a valid biorthogonal wavelet.

3. WAVELETS IN HIGHER DIMENSIONS

The definitions in Chapter 2 deal with wavelets in 1D space, but for many applications of wavelets in computer graphics transformations in 2D or higher dimensions are needed. There are two approaches to extend the wavelet definitions to higher dimensions: One is to apply tensor products of 1D wavelets and scaling functions. The two methods mentioned in literature are the standard and the nonstandard decomposition. The other method, called dilation matrix method, extends the definition of the wavelet and scaling functions by using a dilation matrix instead of a simple factor.

3.1 Standard Decomposition

The standard wavelet basis functions, in 2D also called rectangular wavelet basis functions, are generated through the cartesian product of the 1D wavelet basis functions or the mother scaling function $\phi_{0,0}$ in every dimension. In the 2D case, the standard basis functions are:

$$\begin{aligned}
\phi(x, y) &= \phi_{0,0}(x)\phi_{0,0}(y) \\
\left. \begin{aligned}
{}^{R1}\psi_{j,k}(x, y) &= \psi_{j,k}(x)\phi_{0,0}(y) \\
{}^{R2}\psi_{j,k}(x, y) &= \phi_{0,0}(x)\psi_{j,k}(y) \\
{}^{R3}\psi_{j,m,k,n}(x, y) &= \psi_{j,k}(x)\psi_{m,n}(y)
\end{aligned} \right\} \begin{aligned}
0 \leq j, m < L \\
0 \leq k < 2^j \\
0 \leq n < 2^m
\end{aligned} \tag{15}
\end{aligned}$$

$\phi(x, y)$ denotes the 2D scaling function and the different types of wavelet functions are defined as ${}^{R1}\psi_{j,k}(x, y)$, ${}^{R2}\psi_{j,k}(x, y)$ and ${}^{R3}\psi_{j,m,k,n}(x, y)$.

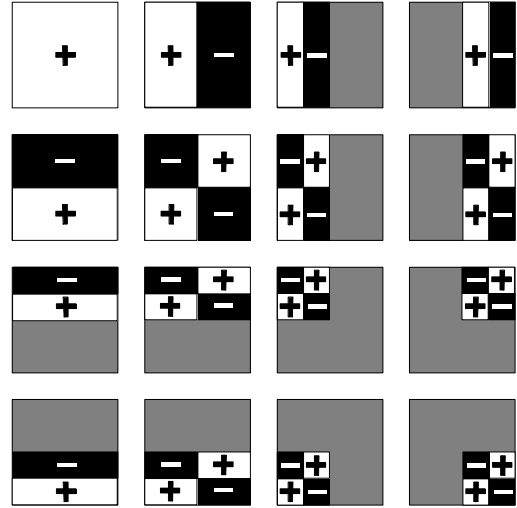


Figure 1: 2D standard Haar wavelet basis

Fig. 1 shows the 2D standard Haar basis functions for a 4x4 image: It contains one scaling function in the upper left corner, three ${}^{R1}\psi_{j,k}(x, y)$ wavelets on the upper border, three ${}^{R2}\psi_{j,k}(x, y)$ wavelets on the left border and the remaining nine ${}^{R3}\psi_{j,m,k,n}(x, y)$ wavelets.

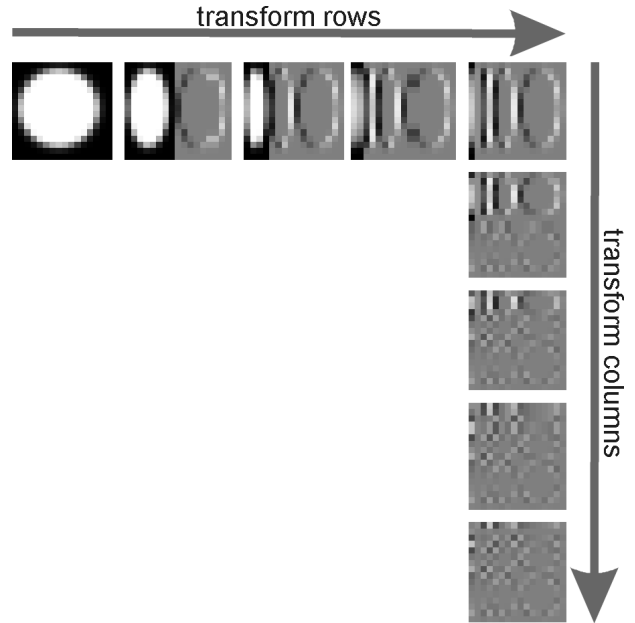


Figure 2: 2D standard decomposition

The fast wavelet transformation with the standard basis wavelets, also known as standard decomposition, is computed by successively applying the 1D wavelet transformation to the data in every dimension. In the 2D case, all the rows are

transformed first, then a 1D wavelet transformation is applied on all columns of the intermediate result. Fig. 2 illustrates the rectangular decomposition. The wavelet coefficients of the 1D transformation steps are stored in the right (row transform) or lower (column transform) part, the scaling coefficients in the left or upper part, respectively. Note that the wavelet coefficients can also have negative values - therefore the value zero of a wavelet coefficient is displayed as 50% gray.

3.2 Non-Standard Decomposition

The nonstandard wavelet basis functions, in 2D also called square wavelet basis functions, are generated through the cartesian product of 1D wavelets and 1D scaling functions. In contrast to the standard basis functions, the non-standard basis functions always use tensor products of wavelet and/or scaling functions of the same resolution level. In the 2D case, the nonstandard basis functions are:

$$\begin{aligned} \phi(x, y) &= \phi_{0,0}(x)\phi_{0,0}(y) \\ \left. \begin{aligned} {}^h\psi_{k,m}^j(x, y) &= \psi_{j,k}(x)\phi_{j,m}(y) \\ {}^v\psi_{k,m}^j(x, y) &= \phi_{j,k}(x)\psi_{j,m}(y) \\ {}^d\psi_{k,m}^j(x, y) &= \psi_{j,k}(x)\psi_{j,m}(y) \end{aligned} \right\} \begin{aligned} 0 \leq j < L \\ 0 \leq k, m < 2^j \end{aligned} \quad (16) \end{aligned}$$

Like in the standard decomposition, it contains one 2D scaling function and three different types of 2D wavelet functions. Note that the wavelet functions ${}^d\psi_{k,m}^j(x, y)$ are a subset of the wavelet functions ${}^R\psi_{j,m,k,n}(x, y)$ in the rectangular decomposition.

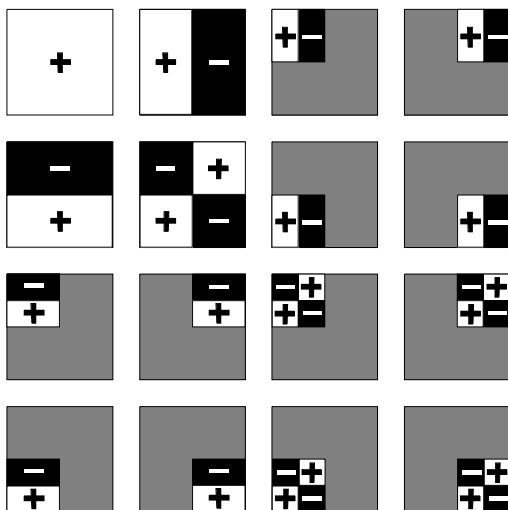


Figure 3: 2D non-standard Haar wavelet basis

Fig. 3 shows the 2D non-standard Haar basis functions for a 4x4 image with one scaling function,

five ${}^h\psi_{k,m}^j(x, y)$ wavelets in the upper part, five ${}^v\psi_{k,m}^j(x, y)$ wavelets in the left part and five ${}^d\psi_{k,m}^j(x, y)$ wavelets in the remaining positions.

The non-standard wavelet decomposition can be computed with a similar technique as the standard decomposition: A 1D wavelet transformation step - not the whole wavelet transformation as in the rectangular decomposition - is applied in every dimension. This generates $(2^{\dim} - 1)$ subbands with wavelet coefficients and one subband with scaling coefficients. This transformation scheme is applied recursively on the scaling coefficients until the lowest level is reached (Fig. 4).

The non-standard decomposition is slightly more efficient to compute than the standard decomposition: For an $m \times m$ image only $(8/3)(m^2 - 1)$ assignments are needed, compared to $4(m^2 - m)$ in the standard decomposition. Also the compression ratios are usually better for the square decomposition, because the support of the wavelet functions are square and support widths of the wavelet basis functions are lower or equal than their counterparts in the rectangular decomposition and therefore they exploit more locality.

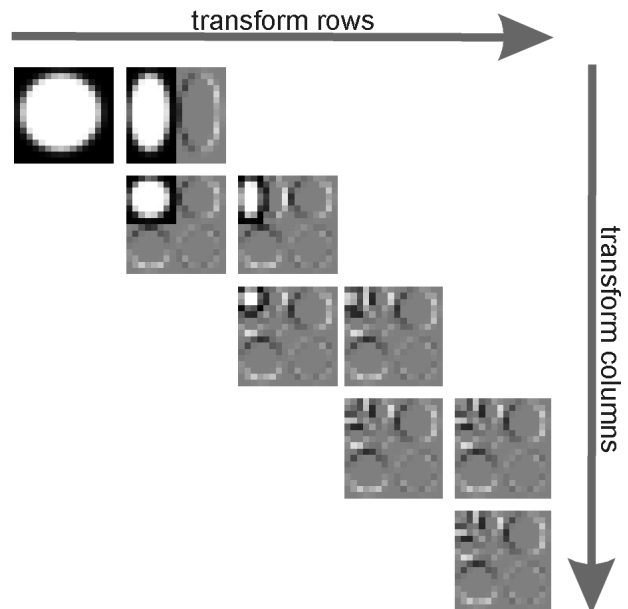


Figure 4: 2D non-standard decomposition

3.3 Quincunx and other Dilation Matrix Methods

One alternative way to extend the formulas to 2D is to directly use 2D wavelets and 2D scaling functions

with a dilation matrix D in Eq. 2 as described in [Kovac92], instead of the simple dilation factor 2. The wavelets and scaling functions can be computed from their mother 2D wavelet and mother 2D scaling function by:

$$\begin{aligned} \phi_{n,\bar{k}}(\bar{x}) &:= \phi(D^n \bar{x} - \bar{k}) \\ \psi_{n,\bar{k}}(\bar{x}) &:= \psi(D^n \bar{x} - \bar{k}) \end{aligned} \quad (17)$$

with $\bar{k} = (k_1, \dots, k_{dim})$; $k_i = 0, \dots, 2^n - 1$; $1 \leq i \leq dim$

The quincunx scheme is one of these dilation matrix methods in 2D with the property $DZ^2 = \{(x,y); x+y \in 2Z\}$. The most promising dilation matrix for the quincunx scheme is $D = \begin{pmatrix} 1 & 1 \\ 1 & -1 \end{pmatrix}$.

One drawback of this method is the higher computational cost of the wavelet transformation: n -dimensional filters have to be applied instead of 1D filters in the separable methods. Because of this drawback, it is rarely used in the application of wavelets to computer graphics.

4. INTERLEAVED DIMENSION DECOMPOSITION

In this chapter a new type of separable wavelets for higher dimensions based on tensor products of 1D wavelets called interleaved dimension decomposition is introduced. The wavelet functions of the interleaved dimension decomposition in N dimensions are generated by the tensor products of a 1D wavelet function of level j in the d^{th} dimension with 1D scaling functions of level j in the dimensions up to $d-1$ and 1D scaling functions of level $j+1$ in the dimensions higher than d . The higher dimensional scaling function for the interleaved dimension basis is the same as in the standard and non-standard basis. The interleaved dimension basis functions in 2D are defined by:

$$\begin{aligned} \phi(x, y) &= \phi_{0,0}(x)\phi_{0,0}(y) \\ \left. \begin{aligned} {}^{xy}\psi_{k,n}^j(x, y) &= \psi_{j,k}(x)\phi_{j+1,n}(y) \\ {}^y\psi_{k,m}^j(x, y) &= \phi_{j,k}(x)\psi_{j,m}(y) \end{aligned} \right\} \begin{aligned} 0 \leq j < L \\ 0 \leq k, m < 2^j \\ 0 \leq n < 2^{j+1} \end{aligned} \end{aligned} \quad (18)$$

The different wavelet functions are indexed in the left superscript by the dimension of the 1D wavelet function followed by the dimensions with the 1D scaling functions of the higher level. Therefore the superscript xy of the wavelet in Eq. 18 denotes a tensor product of a 1D wavelet in x -direction and a 1D scaling function in y -direction of a level one higher than the 1D wavelet.

Note that the decomposition is dependent on the ordering of the dimensions. In 2D there are two possible permutations. Therefore the second possible choice of the basis functions in 2D is:

$$\begin{aligned} \phi(x, y) &= \phi_{0,0}(x)\phi_{0,0}(y) \\ \left. \begin{aligned} {}^{yx}\psi_{k,n}^j(x, y) &= \phi_{j+1,k}(x)\psi_{j,n}(y) \\ {}^x\psi_{k,m}^j(x, y) &= \psi_{j,k}(x)\phi_{j,m}(y) \end{aligned} \right\} \begin{aligned} 0 \leq j < L \\ 0 \leq k, m < 2^j \\ 0 \leq n < 2^{j+1} \end{aligned} \end{aligned} \quad (19)$$

Without loss of generality, we will refer to the first permutation in the 2D case defined in Eq. 18 - analog assumptions can be made with the 2D wavelet basis in Eq. 19. Fig. 5 shows the 2D interleaved dimension Haar basis functions for a 4x4 image from Eq. 18:

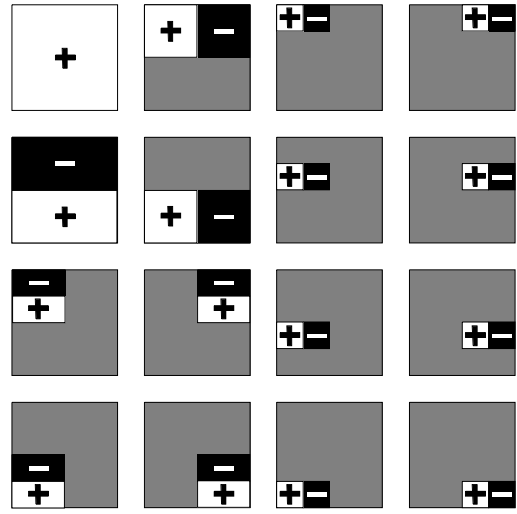


Figure 5: 2D interleaved dimension Haar basis

The wavelets ${}^{xy}\psi_{k,n}^j(x, y)$ are the same as the wavelets ${}^y\psi_{k,m}^j(x, y)$ in the non-standard decomposition. Therefore one third of the wavelet functions and also wavelet coefficients of the non-standard decomposition in 2D are identical to the functions and coefficients of the interleaved dimension decomposition. This can be seen by the comparison of Fig. 4 and Fig. 5, where five functions on the lower left corner are matching. But except one wavelet function on the lowest multiresolution level, there is no match of wavelets of the interleaved dimension decomposition with the standard decomposition. While most of the standard wavelet functions are tensor products of 1D wavelets, the interleaved dimension wavelet functions are tensor products of exactly one 1D wavelet function in one dimension and 1D scaling functions in all other dimensions.

The number of different types of wavelet functions of the interleaved dimension decomposition is equal the number of dimensions dim , while the standard and the non-standard decomposition use $2^{\text{dim}-1}$ different types of wavelet functions. So in 3D we get a basis with one smooth function and three wavelets - compared to seven types of wavelets for the standard and non-standard decomposition. If we use sequential ordering of the dimensions we get in 3D the basis functions:

$$\begin{aligned}\phi(x, y, z) &= \phi_{0,0}(x)\phi_{0,0}(y)\phi_{0,0}(z) \\ {}^{xyz}\psi_{k,n,m}^j(x, y, z) &= \psi_{j,k}(x)\phi_{j+1,n}(y)\phi_{j+1,m}(z) \\ {}^{yz}\psi_{k,o,n}^j(x, y, z) &= \phi_{j,k}(x)\psi_{j,o}(y)\phi_{j+1,n}(z) \\ {}^z\psi_{k,o,p}^j(x, y, z) &= \phi_{j,k}(x)\phi_{j,o}(y)\psi_{j,p}(z) \\ \dots &\text{with } 0 \leq j < L; 0 \leq k, o, p < 2^j; 0 \leq n, m < 2^{j+1}\end{aligned} \quad (20)$$

The interleaved dimension decomposition is very similar to the non-standard decomposition: One 1D wavelet transformation step is applied to the first dimension. But contrary to the nonstandard decomposition only the resulting scaling coefficients are transformed with the following 1D transformation steps, not the wavelet coefficients as in the non-standard decomposition. The transformation steps are cycled in the different dimensions until only one scaling coefficient remains. It is easy to see, that all the intermediate scaling coefficients are the same as in the non-standard decomposition. Fig. 6 illustrates the interleaved dimension decomposition in 2D.

The interleaved dimension decomposition can be seen as an incomplete non-standard decomposition, like it is shown in [Kopp96] that the non-standard decomposition can be viewed as an incomplete standard decomposition. Therefore also the number of operations needed for the decomposition is lower than in the other decompositions: The interleaved dimension needs only $2(m^2-1)$ assignments compared to $4(m^2-m)$ and $(8/3)(m^2-1)$ assignments for the standard and the nonstandard decomposition. This efficiency of the calculation is made at the cost that the multidimensional wavelets contain only in one dimension a 1D wavelet component. Therefore for compression issues, coherence is only exploited in one dimension leading to a worse compression rate in most of the cases.

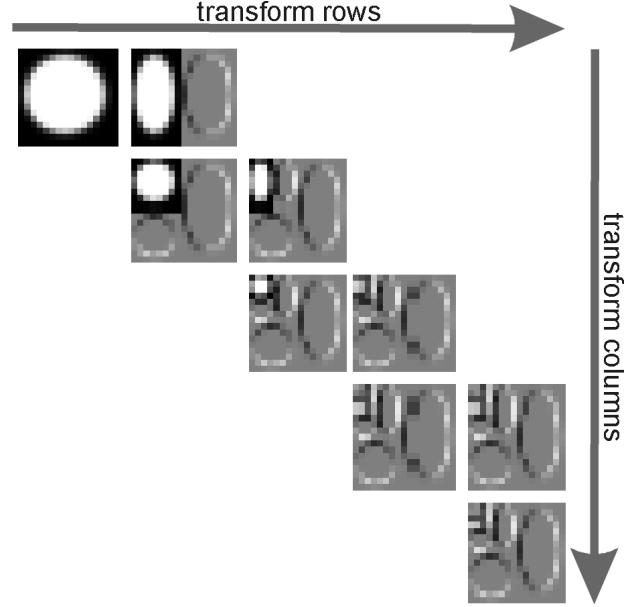


Figure 6: 2D interleaved dimension decomposition

It is mentioned in [Daube92] that the non-standard decomposition can be generated from an extension of the multiresolution concept to higher dimensions. The interleaved dimension decomposition is an alternative for multiresolution approaches in higher dimensions: The higherdimensional multiresolution spaces \mathbf{V}^j and \mathbf{W}^j and the multidimensional scaling functions are the same. One of the $(2^{\text{dim}-1})$ different wavelet functions of the nonstandard decomposition remains the same while the others are replaced with $\text{dim}-1$ sets of translated, more local wavelets. An interesting feature of the interleaved dimension decomposition is the ability to generate $\text{dim}-1$ intermediate multiresolutions - let us demonstrate this property with wavelets in 3D in the ordering of Eq. 20:

$$\begin{aligned}\mathbf{V}^0 &\subset \mathbf{V}^{0,z} \subset \mathbf{V}^{0,yz} \subset \mathbf{V}^1 \subset \mathbf{V}^{1,z} \subset \mathbf{V}^{1,yz} \subset \mathbf{V}^2 \subset \dots \\ \mathbf{V}^j &= \mathbf{V}^j \otimes \mathbf{V}^j \otimes \mathbf{V}^j \\ \mathbf{V}^{j,z} &= \mathbf{V}^j \otimes \mathbf{V}^j \otimes \mathbf{V}^{j+1} = \mathbf{V}^j \oplus \{ {}^z\psi_{k,o,p}^j(x, y, z) \} \\ \mathbf{V}^{j,yz} &= \mathbf{V}^j \otimes \mathbf{V}^{j+1} \otimes \mathbf{V}^{j+1} = \mathbf{V}^{j,z} \oplus \{ {}^{yz}\psi_{k,o,n}^j(x, y, z) \} \\ \mathbf{V}^{j+1} &= \mathbf{V}^{j,yz} \oplus \{ {}^{xyz}\psi_{k,n,m}^j(x, y, z) \}\end{aligned} \quad (21)$$

The corresponding wavelet spaces \mathbf{W}^j , $\mathbf{W}^{j,z}$ and $\mathbf{W}^{j,yz}$ can be built by orthogonal complement. The area/volume/hypervolume dilation from one intermediate level to the next is only 2 compared to 2^{dim} for the non-standard decomposition.

5. APPLICATIONS TO COMPUTER GRAPHICS

A detailed discussion of the different applications, where the interleaved dimension decomposition performs better than the standard or non-standard decomposition is out of scope of this paper. But the following examples sketch applications, where the new decomposition have better performance or generate better quality than the other decompositions.

5.1 Lossless Compression

The interleaved dimension decomposition exploits coherence only in one direction, thus the application to lossy image and volume compression and related applications like image searching [Jacob95] are expected to perform worse than with other decompositions. But the interleaved dimension decomposition can be used to improve lossless compression. The Reversible-Two-Six (RTS) wavelet introduced by [Zandi95] is the most promising one for the application of lossless compression. In one transformation step of the RTS wavelet in 1D, the resulting scaling coefficients of the lower level have the same precision as the scaling coefficients of the higher level, while the range of possible 1D wavelet coefficients is about three times as big as the range of the scaling coefficients. Applying the non-standard decomposition in 2D results in 2/3 of the wavelet coefficients in the value range three times of the original data and 1/3 of the wavelet coefficients in a ninefold value range, while the interleaved dimension decomposition needs only a threefold value range for all wavelet coefficients. Since all possible coefficient values must be handled by the entropy coder, the interleaved dimension decomposition performs sometimes better than the non-standard decomposition. It is shown in chapter 4, that the interleaved dimension decomposition can be seen as an incomplete non-standard decomposition. Therefore the adaptive basis selection in [Kopp96] can be extended with the interleaved dimension decomposition.

5.2 Multiresolution Imaging

Multiresolution images do not have a fixed pixel size, but the resolution varies over the image. An efficient way to implement multiresolution images in a paint system uses wavelets as a representation of the images. [Berma94] utilize a quadtree structure with three Haar wavelet coefficients of the nonstandard decomposition in each node. The display of the multiresolution image is achieved by traversing the quadtree in the specified display region by applying an inverse 2D decomposition step. It is easy to see that the interleaved dimension decomposition can speed up this procedure because less assignments are needed to compute. Also the update from the current level, where the user is painting, to the coarser ones

can be done faster with the interleaved dimension decomposition.

5.3 2D and 3D Morphing

The calculation of an intermediate images in image morphing algorithms is done in three steps: firstly the determination of feature correspondence and of an intermediate feature geometry, secondly the warping of the source and the destination images to intermediate images that match the feature geometry, and finally the blending of the two warped images. [Kopp97] uses wavelets for the blending with different blending factors for different multiresolution levels. This gives the animator the possibility to introduce a disparity between the morphing of global and detail features that can lead to interesting new effects. The additional intermediate multiresolution levels of the interleaved dimension decomposition provide a better image quality of the resulting morphing sequence, since the transition of one level to the next has only an area dilation factor of 2 compared to 4 in the non-standard decomposition.

An other problem occurs with volume morphing: If the morphing is done in spatial domain, distracting high frequency distortions occur in the intermediate volumes. In [He94] this problem is avoided by applying the morphing in the wavelet domain with the non-standard decomposition. In the intermediate volumes the wavelets of the higher levels, which correspond to the high frequencies, are faded off. A problem with this approach is the blocking artifact, which reveals the alignment of the coordinate axes on the intermediate volume. The intermediate multiresolution levels of the interleaved dimension decomposition makes the fading off of the higher levels more smoothly, therefore the blocking artifact is less visible.

6. CONCLUSION

A new wavelet decomposition called interleaved dimension decomposition was introduced. The comparison with the standard and non-standard decomposition showed some interesting aspects: The interleaved dimension decomposition is faster to generate, exploits more locality and builds - like the non-standard decomposition - higherdimensional multiresolution spaces. But unlike the non-standard decomposition, intermediate multiresolution spaces can be built. The interleaved dimension decomposition can be used to improve some wavelet based computer applications. Some examples were sketched in this paper including lossless compression, multiresolution imaging, and morphing in 2D and 3D.

REFERENCES

- [Berma94] Berman, D., Bartell, J., Salesin, D.: Multiresolution Painting and Compositing, *Computer Graphics, Annual Conference Series (Siggraph'94 Proceedings)*, pp. 85-90, 1994
- [Daube92] Daubechies, I.: *Ten Lectures on Wavelets*, Vol. 61 of CBMS-NSF Regional Conference Series in Applied Mathematics, SIAM, Philadelphia, PA 1992
- [Eck95] Eck, M., DeRose, T., Duchamp, T., Hoppe, H., Lounsberry, M., Stuetzle, W., Multiresolution Analysis of Arbitrary Meshes, *Computer Graphics, Annual Conference Series (Siggraph'95 Proceedings)*, pp. 173-182, 1995
- [Finke94] Finkelstein, A., Salesin, D.: Multiresolution Curves, *Computer Graphics, Annual Conference Series (Siggraph'94 Proceedings)*, pp. 261-268, 1994
- [Glass95] Glassner, A. S.: *Principles of Digital Image Synthesis*, Morgan Kaufmann Publishers Inc., Volume 1, pp. 243-298, 1995
- [Gortl93] Gortler, S., Schröder, P., Cohen, M., Hanrahan, P., Wavelet Radiosity, *Computer Graphics, Annual Conference Series (Siggraph'93 Proceedings)*, pp. 221-230, 1993
- [He94] He, T., Wang, S., Kaufmann, A.: Wavelet-Based Volume Morphing. *Proceedings Visualization '94*, Washington DC, IEEE Computer Society Press, pp. 85-92, 1994
- [Jacob95] Jacobs, C., Finkelstein, A., Salesin, D.: Fast Multiresolution Image Querying, *Computer Graphics, Annual Conference Series (Siggraph'95 Proceedings)*, pp. 277-286, 1995
- [Kopp96] Kopp, M., Lossless Wavelet Based Image Compression with Adaptive 2D Decomposition, *Proceedings of the Fourth International Conference in Central Europe on Computer Graphics and Visualization 96 (WSCG96)*, pp. 141-149, Plzen, 1996.
- [Kopp97] Kopp, M., Purgathofer, W., Multiresolution Image Morphing, Technical Report TR-186-2-97-20, Institute of Computer Graphics, Vienna University of Technology, 1997
- [Kovac92] Kovacevic, J., Vetterli, M.: Nonseparable Multidimensional Perfect Reconstruction Filter Banks and Wavelet Bases for \mathbb{R}^n , *IEEE Trans. Information Theory*, Vol. 38, No. 2, pp. 533-555, March 1992
- [Lippe95] Lippert, L., Gross, M.: Fast Wavelet Based Volume Rendering by Accumulation of Transparent Texture Maps, *Eurographics'95 Conference Proceedings, Computer Graphics Forum* Vol. 14, Nr. 3, pp. 431-443, 1995
- [Liu94] Liu, Z., Gortler, S., Cohen, M.: Hierarchical Spacetime Control, *Computer Graphics, Annual Conference Series (Siggraph'94 Proceedings)*, pp. 35-42, 1994
- [Schrö95] Schröder, P., Sweldens, W.: Spherical Wavelets: Efficiently Representing Functions on a Sphere, *Computer Graphics, Annual Conference Series (Siggraph'95 Proceedings)*, pp. 161-172, 1995
- [Shapi93] Shapiro, J. M.: Embedded Image Coding using Zerotrees of Wavelet Coefficients, *IEEE Transactions on Signal Processing*, Vol. 41, Nr. 12, pp 3445-3462, 1993
- [Zandi95] Zandi, A., Allen, J. D., Schwartz, E. L., Boliek, M., *IEEE Data Compression Conference, Snowbird, UT*, March 1995